

DMRG Approach to Optimizing Two-Dimensional Tensor Networks

Katharine Hyatt and E.M. Stoudenmire

*Center for Computational Quantum Physics,
Flatiron Institute, New York, NY 10010 USA*

(Dated: June 5, 2022)

Tensor network algorithms have been remarkably successful solving a variety of problems in quantum many-body physics. However, algorithms to optimize two-dimensional tensor networks known as PEPS lack many of the aspects that make the seminal density matrix renormalization group (DMRG) algorithm so powerful for optimizing one-dimensional tensor networks known as matrix product states. We implement a framework for optimizing two-dimensional PEPS tensor networks which includes all of steps that make DMRG so successful for optimizing one-dimension tensor networks. We present results for several 2D spin models and discuss possible extensions and applications.

Introduction—Since the development of the density matrix renormalization group algorithm (DMRG) [1–3] and its description in terms of matrix product state tensor networks (MPS) [4–6], tensor networks have become an important technique in the study of quantum systems [7, 8]. In addition to underpinning powerful numerical algorithms, tensor networks are also naturally suited to theoretical analysis, leading to significant advances in understanding strongly-correlated quantum systems [9–11]. With the advent of time-dependent [12, 13], and finite-temperature methods for MPS [14, 15], the applicability of tensor network methods has broadened beyond the equilibrium and low-energy settings. Just as importantly, significant progress has been made in extending these methods to 2D systems in a scalable way, primarily through the development of 2D tensor networks known as projected entangled pair states (PEPS) [16–18].

Methods for optimizing PEPS tensor networks have become quite sophisticated. The most common application of PEPS is finding ground states of two-dimensional (2D) quantum systems of infinite size [19, 20]. The resulting infinite PEPS (iPEPS) methods give state-of-the-art results for challenging spin and fermion models [21–29]. Finite-size PEPS also remain a popular choice [30–35], and can be necessary, such as when translation invariance symmetry is absent. Recent applications of finite PEPS even include spin-glass systems [36] and tensor completion problems involving image data [37].

One common technique for optimizing finite

or infinite PEPS is to use imaginary time evolution [19]. Faster algorithms have also been implemented based on conjugate gradient optimization [38] or the iterative solution of a generalized eigenvalue problem [39]. While these algorithms extend many compelling aspects of the DMRG and MPS approach to solving 2D problems scalably, they also omit certain aspects that make DMRG an especially powerful algorithm.

The specific aspects which make the DMRG algorithm so powerful are (1) the preservation of the MPS canonical form throughout the algorithm, where all the MPS tensors except the ones being optimized encode an orthonormal basis; (2) the optimization of the MPS tensors through solving a regular (not generalized) eigenvalue problem using fast, iterative solvers such as Davidson or Lanczos; and (3) the freedom to make large updates to individual tensors while maintaining overall stability. These aspects, taken together, allow DMRG to translate the very rapid convergence of iterative eigen-solvers into a method for optimizing an entire tensor network. In the very best cases (one-dimension systems with a sizeable gap), one can observe exponentially fast convergence with the number of DMRG sweeps over the system.

In what follows, we demonstrate an algorithm for optimizing PEPS ground states which realizes all three of the important technical aspects of DMRG listed above. A key ingredient in our work is a recent advance in obtaining canonical forms for PEPS tensor networks and a description of their properties [40], a concept also re-

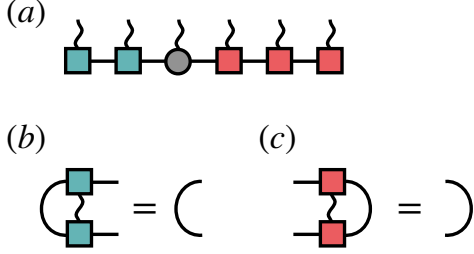


FIG. 1: Illustration of (a) a matrix product state (MPS) tensor network in canonical form with respect to the third site, with tensors to the left obeying the (b) left-canonical condition and tensors to the right obeying the (c) right-canonical condition. Curly lines represent physical or site indices of tensors.

cently explored in Ref. 41. However, we take a different approach from Refs. 40 and 41 for carrying out the canonization at each step, raising the interesting question of which approach is best and underscoring how the efficiency and accuracy of the DMRG optimization we present will certainly continue to improve with further research.

Overview of DMRG Algorithm for MPS—To set the stage for our algorithm for optimizing 2D PEPS tensor networks, let us first review what is essentially the same algorithm—the density matrix renormalization group (DMRG)—for optimizing an MPS ground-state wavefunction. We will describe the one-site DMRG algorithm. Although the more common two-site DMRG algorithm has the advantage of allowing the MPS bond dimension to be adjusted adaptively, one-site DMRG is simpler to generalize to our two dimensional setting.

The DMRG algorithm begins with an MPS in canonical form with respect to some site j as illustrated in Fig. 1(a), with the figure showing the case $j=3$. By canonical form, one means all MPS tensors to the left of site j obey the left-orthogonality condition Fig. 1(b) and tensors right of j obey the right-orthogonality condition Fig. 1(c). These orthogonality conditions turn out to be crucial for the success of the DMRG algorithm, as each optimization step can be written as a regular eigenvalue problem, making the algorithm numerically stable and efficient. In

our PEPS algorithm, we will employ an analogous canonical form for the same purposes.

To optimize the MPS within one step of the DMRG algorithm, only the center tensor at site j is updated, holding the rest fixed. The terms of the Hamiltonian are projected into the orthonormal basis defined by these fixed, canonical MPS tensors. This projection can be performed efficiently by contracting the MPS tensors one at a time with each other and with the individual operators making up the Hamiltonian.

After projection of each term in the Hamiltonian, one solves for the lowest energy eigenvector of the projected Hamiltonian in order to obtain the updated tensor at site j . For efficiency, the eigenvalue problem is solved using an iterative algorithm such as Lanczos or Davidson. In practice, one does not converge these solvers fully since the basis defined by the rest of the MPS is not yet optimal. The fact that DMRG optimizes each tensor this way is one of its key advantages: iterative eigensolver algorithms converge very rapidly in practice, and because of the orthonormality of the MPS tensors, local improvements directly translate into global improvements.

We will see that all of the steps above can be translated into the context of PEPS optimization. Some steps such as using an iterative eigensolver to optimize each tensor generalize straightforwardly from MPS to PEPS. Other steps such as canonization of tensors can be done optimally for MPS, but are much more challenging for PEPS, and the question of which canonization algorithm is best remains an open question for future research.

For studying two-dimensional systems, DMRG can be applied to quasi-1D ladder-like ($N_x \gg N_y$) lattices, but the bond dimension χ necessary to accurately represent a state must grow exponentially in N_y [42, 43]. Applying DMRG to 2D systems where N_y is much greater than $N_y \approx 10$ while preserving a fixed accuracy is extremely expensive.

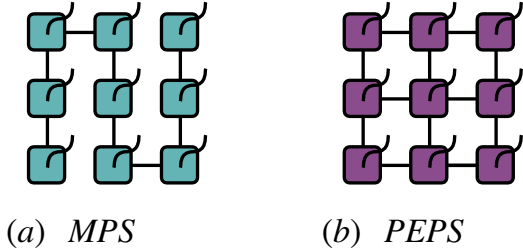


FIG. 2: **2D Tensor Networks:** (a) MPS with snaking pattern and (b) PEPS, both shown for a 3×3 lattice with open boundaries. Curly lines are uncontracted, physical indices.

Projected Pair Entangled States—Projected pair entangled states (PEPS) are a generalization of MPS tensor networks to two-dimensional systems. In an MPS, the virtual indices of each tensor connect to just two neighbors, resulting in a one-dimensional, chain-like network. PEPS tensors carry more virtual indices, typically chosen such that the network of contracted virtual indices mimics the pattern of dominant interactions in the Hamiltonian—see Fig. 2. Like MPS, each tensor in PEPS carries a *physical* index for the physical degrees of freedom on the site. Unlike an MPS which requires an exponentially growing bond dimension to capture ground states of two-dimensional systems of increasing size, PEPS are empirically known to capture ground states using a modest bond dimension ($\chi \sim 10 - 20$) to a fixed accuracy independent of system size for a wide variety of Hamiltonians.

A key difference of PEPS from MPS is that computing observables of a PEPS, such as expected values of local operators, has an exponential cost when performed in a numerically exact way. This difficulty can be traced back to the presence of loops in the contraction pattern of virtual PEPS tensor indices. Fortunately though, observables can be computed accurately and reliably using various approximations. In this work, observables are evaluated by treating the boundary columns of the PEPS as MPS tensor networks, the interior columns as matrix product operator (MPO) networks, and by using standard MPO-MPS multiplication techniques to evaluate the contraction of the two, generating a new MPS which represents the contraction up to the first interior column. This can be

repeated to (approximately) contract the entire PEPS. For more detailed information, see the Supplementary Material.

One popular mode of using PEPS exploits translational invariance and parameterizes the ground state of an infinite system by repeating a small unit cell of PEPS tensors. The resulting infinite PEPS (iPEPS) method then has the benefit of avoiding finite-size and boundary effects. However, there are important drawbacks too: iPEPS requires translation invariance, and simulation of lattices without a square geometry is not always straightforward [44]. And very sophisticated algorithms must be developed to account for the Hamiltonian terms acting outside of the particular tensor being optimized, while still ensuring translation invariance.

Here we instead choose to work with finite PEPS with open boundary conditions. Having an edge, and also not having to deal with translation-invariance constraints provides a great technical simplification for the DMRG algorithm we will develop.

Canonization of PEPS—Unlike MPS with open boundary conditions, PEPS has internal closed loops which preclude a scheme in which the exact normalization matrix, \mathcal{N} , constructed by contracting all the tensors when computing the overlap $\langle \psi | \psi \rangle$ *except* the tensors to be optimized, is equal to the identity. However, DMRG-like schemes can be constructed which achieve $\mathcal{N} \simeq \mathbb{I}$ for a faithful representation of the PEPS with very small error [7]. One can also construct schemes in which $\mathcal{N} = \mathbb{I}$ exactly by throwing away some information about the PEPS during the canonization step. Here we develop the latter type of scheme, keeping in mind that it is not unique and may not be optimal – other canonization schemes for PEPS are possible [40, 41].

As the simulation proceeds, the tensors in the column which was just optimized are “canonized” before proceeding to optimize the next column. The canonization procedure takes as input a single column of the PEPS and outputs a new column Q which is unitary and carries the physical indices, and a non-unitary remainder R . The unitary piece Q carries the physical indices and will replace the optimized column. The non-unitary piece R is multiplied into the

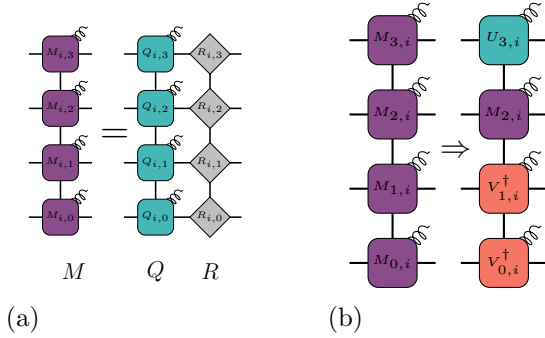


FIG. 3: Canonization (a) of an entire PEPS column to shift to a different column and (b) canonization within a specific PEPS column.

next column to be optimized and has only virtual indices. Fig. 3 illustrates the canonization procedure. This procedure comes with a guarantee that Q is always exactly canonical, but the product of Q times R may not exactly reconstruct the original, input column because the optimization involved may not reach its global minimum.

To briefly outline the canonization procedure (see the Supplemental Material for more details): we use the input column A as an initial guess for Q , and compute $\text{Tr}[A^\dagger Q Q^\dagger A]$, leaving one tensor of Q (but not Q^\dagger) uncontracted. The resulting tensor is called the environment tensor. We then compute a polar decomposition of this environment, which gives an updated Q tensor which is unitary and has maximal overlap with the environment [45]. Having updated all Q , we compute $R = Q^\dagger A$ and determine the inner product of QR with A . Once the inner product is high enough (> 0.99 in our simulation) the canonization procedure is complete. This method is not unique, and it may not generate the optimal canonical representation of an input column in terms of minimizing the bond dimension of the resulting columns of orthogonal Q and remainder R tensors. However it does have the advantage that the Q tensors replacing the input column are exactly orthogonal by construction, so that the canonization succeeds as long as the product of QR with A is close enough to one.

The goal of our approach is to implement an analogue of DMRG for PEPS. Above we discussed the first step of translating the gauging scheme from single MPS tensors to entire

PEPS columns. Even after implementing the inter-column canonization, finding the ground state would still require solving a generalized eigenvalue problem, $\hat{H}v - \lambda \hat{N}v = 0$ (\hat{N} is the normalization matrix). To solve this final obstacle we extend the scheme one step further. One can also canonize *within* a column, ensuring the correct normalization conditions above and below a specific tensor, given that the left and right environments are also properly canonized. An example is shown in Fig. 3b. Just as in DMRG, this is done with an SVD or QR decomposition of the tensors above and below, making this canonization step optimal and guaranteed to succeed. This further step is performed before optimization and is useful because the optimization can now be expressed as a *regular* eigenvalue problem $\hat{H}v = \lambda v$, which is more efficient to solve and more numerically stable. Just as in 1D DMRG, we use an iterative eigensolver (Davidson) to optimize the local tensor, rather than fully diagonalizing the Hamiltonian in the local basis.

Application to the Heisenberg Model—To test the reliability of the method, we simulate the spin 1/2 Heisenberg model on the square lattice, whose Hamiltonian is:

$$\hat{H} = \sum_{\langle i,j \rangle} \hat{S}_i^x \hat{S}_j^x + \hat{S}_i^y \hat{S}_j^y + \hat{S}_i^z \hat{S}_j^z \quad (1)$$

where $\langle i,j \rangle$ means sites i and j are nearest-neighbors. This model has also been extensively studied as a test-bed for PEPS algorithms [20, 22, 30, 38, 39, 46].

We study system sizes (L, L) with $L = 4, 6, 8, \dots, 16$. The initial parameters in the PEPS are determined randomly, then the PEPS is optimized for 50 sweeps of DMRG, where a sweep means a full pass over every PEPS tensor. We compare the energy per site and the nearest-neighbor spin-spin correlators throughout the simulation, comparing the energy with QMC and DMRG and the correlators with DMRG. We allow the DMRG calculations to use an MPS bond dimension up to 1000, since this is a value that can get good accuracy for the Heisenberg model up through about $L \leq 18$. Beyond a certain size L , DMRG with any fixed bond di-

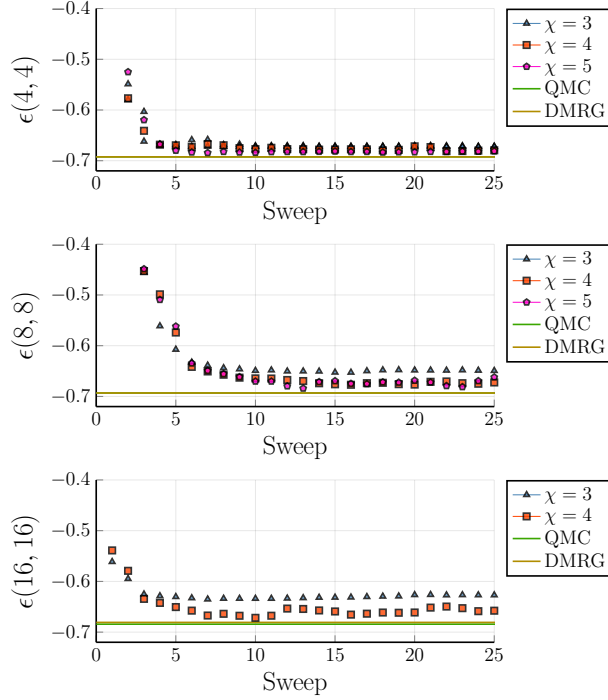


FIG. 4: Energy per site $\epsilon = E/N$ for the Heisenberg model on finite square lattices. In addition to PEPS results, we show quantum Monte Carlo (QMC) and MPS-DMRG results for various finite square lattice sizes. QMC results should be considered exact. All MPS-DMRG results shown used a maximum MPS bond dimension of 1000. Color and symbol shapes indicate PEPS bond dimensions χ .

mension starts to lose accuracy exponentially quickly.

Progress towards the ground state is initially accelerated by performing simple update sweeps of the system for only the first several sweeps, before switching to eigensolver optimization as in DMRG. Once the eigensolver is used, no more simple update steps are performed. The energy traces for the PEPS are presented in Fig. 4. One may ask why occasional increases in energy are seen: this occurs because the canonization process does not always converge to a sufficiently close approximation to the original non-canonical column, and in such cases replacing the column with the canonical version usually causes the energy to increase. This issue is not fundamental to the DMRG approach to optimizing PEPS, however, and will greatly improve with more research into canonization algo-

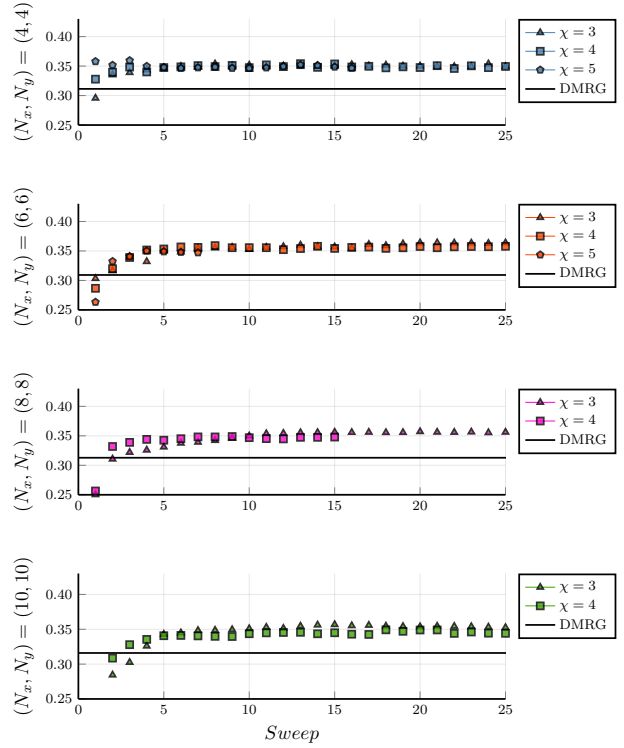


FIG. 5: Summed spin-spin correlators of vertical bonds of the Heisenberg model, and comparison to DMRG with bond dimension 1000. All simulations are run at a 1:1 aspect ratio.

rithms. Also the PEPS energy quickly recovers when such jumps occur.

To further characterize the accuracy of our approach, we compute the nearest-neighbor spin-spin correlator, $\sum_i \langle \vec{S}_i \cdot \vec{S}_{i+1} \rangle / N$ for the center column of the PEPS and compare with DMRG results in Fig. 5. We measure only correlations between nearest vertical neighbors, as this is simplest in our setup. This quantity should allow us to understand how well our algorithm captures quantum fluctuations in the groundstate. Although there is a noticeable disparity between the PEPS results and the DMRG result, which is effectively exact for these system sizes, the difference can be understood as a finite PEPS bond-dimension effect and is comparable to that seen in state of the art iPEPS results [46].

Conclusions—The density matrix renormalization group (DMRG) algorithm, which has proven very powerful for optimizing ground state wavefunctions in the MPS format, can be car-

ried out successfully for PEPS tensor networks, allowing one to scale DMRG to large two-dimensional systems. We have demonstrated that each essential step of DMRG can be performed with very good results.

Among the many interesting 2D interacting Hamiltonians, there are opportunities for our method to either show its usefulness or to suggest avenues for improvements. We found the total run time is dominated by MPO-MPO multiplications (14%) and by tensor contraction (46%). Improvements to existing algorithms for MPO-MPO sums and product would be extremely helpful, and are also an area where the community may be able to make significant progress.

Looking ahead, it will be very interesting to compare the efficiency of optimizing finite PEPS with DMRG versus leading methods for optimizing infinite PEPS (iPEPS), in terms of estimating bulk properties. Note that the finite-size setting of the DMRG algorithm we have implemented is not necessarily a drawback in this comparison, as finite-size effects reveal useful physical information, and the finite setting allows us to make very large updates to each tensor without encountering issues seen in iPEPS optimization due to non-linearity of optimization under translation-invariance constraints.

In terms of future technical developments, our approach would benefit greatly from a better understanding of methods to impose canonical or gauge conditions on PEPS tensors. Open challenges include determining the optimal bond dimensions after canonization and finding more efficient canonization algorithms. PEPS-DMRG would also benefit from improved techniques for approximating the Hamiltonian projection or environment tensors, which could include faster techniques for MPO times MPS products or techniques more specialized to the PEPS-DMRG setting.

The authors wish to especially thank Matthew Fishman for early discussions on canonical forms of PEPS and strategies for optimizing finite PEPS. We also thank Frank Pollman, Michael Zaletel, Garnet Chan, Steve White, and Jing Chen for helpful discussions. All calculations are based on the ITensor Li-

brary [47]. The Flatiron Institute is a division of the Simons Foundation.

-
- [1] S. R. White, Physical review letters **69**, 2863 (1992).
 - [2] S. White, Phys. Rev. B **48**, 10345 (1993).
 - [3] U. Schollwöck, Rev. Mod. Phys. **77**, 259 (2005).
 - [4] S. Östlund and S. Rommer, Physical review letters **75**, 3537 (1995).
 - [5] J. Dukelsky, M. A. Martín-Delgado, T. Nishino, and G. Sierra, EPL (Europhysics Letters) **43**, 457 (1998).
 - [6] U. Schollwöck, Annals of Physics **326**, 96 (2011).
 - [7] R. Orús, Annals of Physics **349**, 117 (2014).
 - [8] E. Stoudenmire and S. R. White, Annual Review of Condensed Matter Physics **3**, 111 (2012).
 - [9] M. B. Hastings, Journal of Statistical Mechanics: Theory and Experiment **2007**, P08024 (2007).
 - [10] X. Chen, Z.-C. Gu, and X.-G. Wen, [Phys. Rev. B](#) **83**, 035107 (2011).
 - [11] F. Pollmann, E. Berg, A. M. Turner, and M. Oshikawa, [Phys. Rev. B](#) **85**, 075125 (2012).
 - [12] A. J. Daley, C. Kollath, U. Schollwöck, and G. Vidal, Journal of Statistical Mechanics: Theory and Experiment **2004**, P04005 (2004).
 - [13] S. R. White and A. E. Feiguin, Physical review letters **93**, 076401 (2004).
 - [14] A. E. Feiguin and S. R. White, Physical Review B **72**, 220401 (2005).
 - [15] S. R. White, Physical review letters **102**, 190601 (2009).
 - [16] G. Sierra and M. Martin-Delgado, [cond-mat/9811170](#).
 - [17] T. Nishino, Y. Hieida, K. Okunishi, N. Maeshima, Y. Akutsu, and A. Gendiar, Prog. Theor. Phys. **105**, 409 (2001).
 - [18] F. Verstraete and J. I. Cirac, cond-mat/0407066 (2004).
 - [19] J. Jordan, R. Orús, G. Vidal, F. Verstraete, and J. I. Cirac, Phys. Rev. Lett. **101**, 250602 (2008).
 - [20] Z.-C. Gu, M. Levin, and X.-G. Wen, [Phys. Rev. B](#) **78**, 205116 (2008).
 - [21] I. Niesen and P. Corboz, [Phys. Rev. B](#) **97**, 245146 (2018).
 - [22] M. Rader and A. M. Läuchli, Physical Review X **8**, 031030 (2018).
 - [23] P. Corboz, T. M. Rice, and M. Troyer, Phys. Rev. Lett. **113**, 046402 (2014).
 - [24] P. Czarnik, M. M. Rams, and J. Dziarmaga,

- Phys. Rev. B **94**, 235142 (2016).
- [25] P. Corboz, P. Czarnik, G. Kapteijns, and L. Tagliacozzo, [Phys. Rev. X **8**, 031031 \(2018\)](#).
 - [26] H.-J. Liao, J.-G. Liu, L. Wang, and T. Xiang, [arxiv:1903.09650 \(2019\)](#).
 - [27] C. Hubig and J. I. Cirac, *SciPost Physics* **6** (2019).
 - [28] P. Czarnik, J. Dziarmaga, and P. Corboz, *Physical Review B* **99**, 035115 (2019).
 - [29] P. Corboz, P. Czarnik, G. Kapteijns, and L. Tagliacozzo, *Physical Review X* **8**, 031031 (2018).
 - [30] M. Lubasch, J. I. Cirac, and M.-C. Bañuls, [Phys. Rev. B **90**, 064425 \(2014\)](#).
 - [31] M. Lubasch, J. I. Cirac, and M.-C. Bañuls, *New Journal of Physics* **16**, 033014 (2014).
 - [32] W.-Y. Liu, S.-J. Dong, Y.-J. Han, G.-C. Guo, and L. He, [Phys. Rev. B **95**, 195154 \(2017\)](#).
 - [33] W.-Y. Liu, S. Dong, C. Wang, Y. Han, H. An, G.-C. Guo, and L. He, [Phys. Rev. B **98**, 241109 \(2018\)](#).
 - [34] L. He, H. An, C. Yang, F. Wang, J. Chen, C. Wang, W. Liang, S. Dong, Q. Sun, W. Han, W. Liu, Y. Han, and W. Yao, [IEEE Transactions on Parallel and Distributed Systems **29**, 2838 \(2018\)](#).
 - [35] S.-J. Dong, C. Wang, Y. Han, G.-c. Guo, and L. He, [Phys. Rev. B **99**, 195153 \(2019\)](#).
 - [36] M. M. Rams, M. Mohseni, and B. Gardas, [arxiv:1811.06518 \(2018\)](#).
 - [37] H. Huang, Y. Liu, and C. Zhu, [arxiv:1903.04735 \(2019\)](#).
 - [38] L. Vanderstraeten, J. Haegeman, P. Corboz, and F. Verstraete, [Phys. Rev. B **94**, 155123 \(2016\)](#).
 - [39] P. Corboz, [Phys. Rev. B **94**, 035133 \(2016\)](#).
 - [40] M. P. Zaletel and F. Pollmann, [arxiv:1902.05100 \(2019\)](#).
 - [41] R. Haghshenas, M. J. O'Rourke, and G. K.-L. Chan, [arxiv:1903.03843](#).
 - [42] S. Yan, D. A. Huse, and S. R. White, *Science*, 1201080 (2011).
 - [43] S. Depenbrock, I. P. McCulloch, and U. Schollwöck, *Physical review letters* **109**, 067201 (2012).
 - [44] S. S. Jahromi, R. Orús, M. Kargarian, and A. Langari, *Physical Review B* **97**, 115161 (2018).
 - [45] G. Evenbly, [Phys. Rev. B **95**, 045117 \(2017\)](#).
 - [46] B. Bauer, G. Vidal, and M. Troyer, *Journal of Statistical Mechanics: Theory and Experiment* **2009**, P09006 (2009).
 - [47] ITensor Library (version 3.0.0) <https://itensor.org>.